

Vibrational Circular Dichroism of Adsorbed Molecules: BINAS on Gold Nanoparticles<sup>†</sup>Cyrille Gautier<sup>‡</sup> and Thomas Bürgi<sup>\*,§</sup>

*Institut de Physique, Laboratoire de Chimie Physique des Surfaces, Université de Neuchâtel, Rue Emile-Argand 11, 2009 Neuchâtel, Switzerland, and Physikalisch-Chemisches Institut, Ruprecht-Karls-Universität Heidelberg, Im Neuenheimer Feld 253, 69120 Heidelberg, Germany*

*Received: November 13, 2009; Revised Manuscript Received: January 19, 2010*

Vibrational circular dichroism (VCD) spectra of small size-selected gold nanoparticles covered by both enantiomers of 1,1'-binaphthyl-2,2'-dithiol (BINAS) were measured. VCD spectra of particles covered by the opposite enantiomers of BINAS show a mirror image relationship. The VCD spectrum of adsorbed BINAS is different from the one of free BINAS and its disulfide form, but it resembles more the dithiol form. Detailed analysis reveals that the angle between the two binaphthyl rings of BINAS is close to 90° for the adsorbed BINAS, similar to what is found for the free molecule. VCD spectra are quite insensitive to the particles size, in contrast to the electronic CD spectra, which change drastically as the particle size increases. This indicates that the vibrational characteristic is a local property. A model of BINAS adsorbed on a Au<sub>10</sub> cluster was used to calculate VCD spectra. As for free BINAS and the disulfide the calculated spectrum of the adsorbed BINAS is in very good agreement with the measured one. This shows the potential of VCD spectroscopy to gain insight into the conformation of chiral molecules adsorbed on small metal particles.

## Introduction

Adsorption of molecules on surfaces is of fundamental importance for many processes comprising separation, (bio)-sensing, surface processing, lubrication, and heterogeneous catalysis. The conformation of the molecules at the surface can have a pronounced effect on surface properties. However, such information is rather difficult to obtain. A special class of surfaces results from modification by chiral molecules. The resulting chirally modified surfaces have potential for applications in enantioselective separation, detection of enantiomers, and heterogeneous enantioselective catalysis.<sup>1,2</sup> The latter effects strongly rely on intermolecular interactions, which depend, among other factors, on the conformation of the adsorbed molecule.<sup>3–7</sup>

A powerful method for obtaining conformational information is vibrational circular dichroism (VCD), i.e., the differential absorption of left- and right-circularly polarized light by a chiral sample.<sup>8</sup> VCD is more sensitive to conformation than conventional infrared absorption spectroscopy. In order to extract that structural information the experimental VCD spectrum has to be compared with theoretical spectra calculated for different conformers. Density functional theory (DFT) calculations have predictive character for VCD spectra of organic molecules.<sup>9</sup> An experimental challenge of VCD spectroscopy is the relatively small signals. The anisotropy factors  $\Delta A/A = \Delta\epsilon/\epsilon$  are typically on the order of  $10^{-4}$  to  $10^{-6}$ . As a consequence measurements on flat surfaces are very challenging, since monolayers typically give rise to absorbance signals of less than  $10^{-2}$ . One way to overcome this obstacle is the use of a high specific surface area material, such as nanoparticles. The latter can be viewed as the nanometer-size analogues of extended flat surfaces. Indeed, we

have shown recently that VCD spectra of molecules adsorbed on small metal particles can be measured.<sup>10,11</sup>

We have prepared in the past gold nanoparticles covered by *N*-acetyl-cysteine<sup>10</sup> and *N*-isobutyryl-cysteine<sup>11</sup> and measured their VCD spectra in D<sub>2</sub>O. We have also calculated VCD spectra of these thiols adsorbed on small gold particles. As expected the calculated VCD spectra strongly depend on the conformation of the thiol and on the way the latter interacts with the gold particle. Comparison between experimental and calculated VCD spectra indicated an adsorption mode where both the *N*-acetyl-cysteine and *N*-isobutyryl-cysteine interact via the thiolate and the carboxylate with the gold particle, in agreement with ATR-IR work and orientation measurements.<sup>12</sup>

The two reports mentioned above are so far the only ones on VCD of molecules adsorbed on metal nanoparticles, to the best of our knowledge. The results are promising, and the technique may become a versatile tool also in view of the fact that chemically modified metal nanoparticles are considered as building blocks in nanotechnology. Compared to VCD of molecules additional aspects may play a role for VCD of molecules adsorbed on metal nanoparticles. For example, the nanoparticles have low-lying electronic states that might have an influence, similar to what was reported for metal complexes.<sup>13</sup> In addition, the electromagnetic field in the vicinity of a metal particle might be amplified, leading to enhanced infrared absorption and possibly enhanced VCD.<sup>14</sup> Also, the role of the structure of the metal particle on the VCD of the adsorbed molecule is unclear. Finally, calculations including metal particles are more difficult, and it is not clear yet if the same quality of agreement between calculations and experiment can be obtained as for free organic molecules. Further examples need to be studied to clarify the importance of these effects.

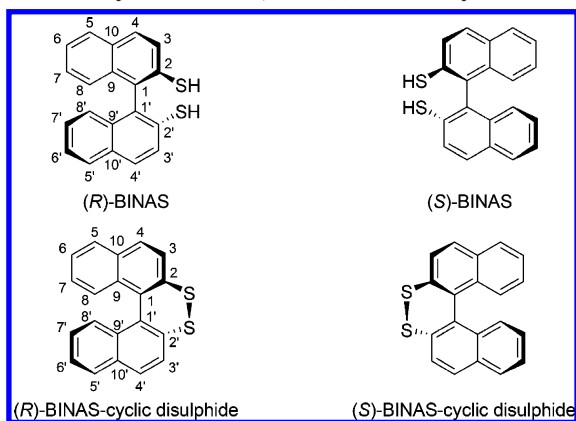
The two systems investigated up to now are challenging for mainly two reasons and are therefore not ideal to learn more about intrinsic aspects of the technique. First of all *N*-acetyl-cysteine and *N*-isobutyryl-cysteine are quite flexible molecules with considerable conformational freedom. Therefore, several

<sup>†</sup> Part of the "Protected Metallic Clusters, Quantum Wells and Metal-Nanocrystal Molecules Symposium" special issue.

\* Corresponding author. Tel: ++49 6221 54 84 75. E-mail: buergi@uni-heidelberg.de.

<sup>‡</sup> Université de Neuchâtel.

<sup>§</sup> Ruprecht-Karls-Universität Heidelberg.

**SCHEME 1: Structure of (R)-BINAS, (S)-BINAS, (R)-BINAS-Cyclic Disulfide, and (S)-BINAS-Cyclic Disulfide**

conformers might contribute to the experimental spectrum. Second, the particles that were studied up to now are soluble in water. It is very likely that water specifically interacts with *N*-acetyl-cysteine and *N*-isobutryl-cysteine via hydrogen bonding and this will influence the VCD at least to a certain extent.<sup>15</sup> This should be included in the calculation of the VCD spectra.

Here we apply VCD spectroscopy to another system with much less conformational freedom and which is soluble in organic solvents, thus avoiding specific intermolecular interactions with the solvent. This should allow us to shed some light on the potential and limitations of the approach. In particular, we have prepared small gold nanoparticles covered with (*R*)-1,1'-binaphthyl-2,2'-dithiol [(*R*)-BINAS] and (*S*)-1,1'-binaphthyl-2,2'-dithiol [(*S*)-BINAS] (see Scheme 1), respectively, and the particles were separated into different sizes by size exclusion chromatography.<sup>16</sup> Then the VCD spectra of the samples were measured and compared with calculated spectra.

## Materials and Methods

The preparation of enantiomerically pure (*R*)- and (*S*)-BINAS was reported elsewhere.<sup>17</sup> Deuterated chloroform (99.8%) and CD<sub>2</sub>Cl<sub>2</sub> (99.9%) were received from Cambridge Isotope Laboratories.

**Spectroscopy.** UV–vis and CD spectra were collected on a Carry 300 and a Jasco 710 spectrometer, respectively. IR and vibrational circular dichroism (VCD) spectra were recorded on a Bruker PMA 50 accessory coupled to a Tensor 27 Fourier transform infrared spectrometer. A photoelastic modulator (Hinds PEM 90) set at 1/4 retardation was used to modulate the handedness of the circular polarized light. Demodulation was performed by a lock-in amplifier (SR830 DSP). An optical low-pass filter (<1800 cm<sup>-1</sup>) in front of the photoelastic modulator was used to enhance the signal/noise ratio. All solutions of BINAS-stabilized gold particles (monolayer protected nanoparticles, MPNs) were prepared in CD<sub>2</sub>Cl<sub>2</sub>. Solutions of (*R*)- and (*S*)-BINAS MPNs, of the corresponding free dithiol and of tetraoctylammonium bromide (TOAB) were prepared in CD<sub>2</sub>Cl<sub>2</sub> with a concentration of 150, 19, and 15 mg mL<sup>-1</sup>, respectively, whereas (*R*)- and (*S*)-BINAS-cyclic disulfide were prepared in CDCl<sub>3</sub> at 25 mg mL<sup>-1</sup>. VCD reference spectra were recorded for racemic mixtures of the samples. Alternatively, the pure solvents served as references.

All spectra were recorded at 10 °C to avoid evaporation of the solvent with a resolution of 8 cm<sup>-1</sup> (4 cm<sup>-1</sup> for BINAS) in a cell equipped with CaF<sub>2</sub> windows and 100, 500, and 1000 μm Teflon spacers for the separated MPNs, BINAS and BINAS-

cyclic disulfide, respectively. Both samples and references were measured for two hours in time slices of 30 min, corresponding to about 16 000 scans in total for sample and reference, respectively. The spectra are presented without smoothing or further data processing.

**Computational Methods.** Density functional theory (DFT) as implemented in Gaussian 03 was used to study the structure of BINAS, BINAS-cyclic disulfide, and BINAS adsorbed on gold particles and to calculate the corresponding IR and VCD spectra. For the gold atoms an effective core potential was used. The calculations were performed using the b3pw91<sup>18,19</sup> functional and a LanL2DZ basis set<sup>20</sup> for Au and a 6-31G(d,p) basis set<sup>21</sup> for all other atoms. Prior to the calculation of the spectra all degrees of freedom were completely relaxed unless otherwise stated. Vibrational frequencies were scaled by a factor of 0.965. IR and VCD spectra were constructed from calculated dipole and rotational strengths assuming Lorentzian band shape with a half-width at half-maximum of 5 cm<sup>-1</sup>. All calculations were performed for the gas phase species.

## Results and Discussion

**Separation and Characterization of the Nanoparticles.** The as prepared BINAS-stabilized gold nanoparticles have an average size smaller than 2 nm as shown by the TEM,<sup>16</sup> which is consistent with the absence of a surface plasmon band at around 520 nm. Nuclear magnetic resonance (NMR) reveals no detectable free BINAS and BINAS-cyclic disulfide in solution. We have reported before<sup>16</sup> that these nanoparticles can be separated according to their size by size exclusion chromatography. Figure 1 shows such a separation. In total five fractions with different color could be separated and were numbered 1–5 according to their elution order or their decreasing size. The observed color-dependence on particle size is a direct consequence of a quantum size effect. The latter is also responsible for the systematic red shift of the absorption onset for increasing particle size. Both the UV–vis and electronic circular dichroism (ECD) spectra change significantly with the size of the particles. These spectra reflect the electronic structure of the particles, which strongly changes with their size in the size regime relevant here. The induction of chirality from chiral adsorbed molecules to metallic nanoparticles has been discussed based on several models during the past decade.<sup>7,10,11,16,22–34</sup> It should be noted that apart from the TEM we do not have direct size/mass information. However, the absorption spectra (and the color of the different fraction) allow one to make some rough estimate of the particle size. Especially, the absorption onset can be compared with the one of thiolate-protected gold particles for which the mass has been determined by mass spectrometry.<sup>27</sup> Therefore our yellow fraction 5 (absorption onset around 400 nm) can be estimated to have 10–15 gold atoms, the green fraction 3 (absorption onset around 700–800 nm) would have 22–25 gold atoms, and the brown fraction 1 (absorption onset above 800 nm) would have 30–40 gold atoms.

**BINAS and BINAS-Cyclic Disulfide.** Before turning our attention to the spectra of the BINAS-stabilized gold particles the vibrational properties of the free ligand are presented. In particular BINAS but also the oxidized cyclic disulfide (BINAS-cyclic disulfide) form were studied. The latter is rigid, whereas the former has three conformational degrees of freedom, namely the two S–H groups and the angle between the naphthyl planes. There is only one minimum for this degree of freedom, whereas there are three possible combinations for the position of the two S–H groups (see Figure 2, both in, both out, one in and one out). The S–H groups pointing inward are slightly more

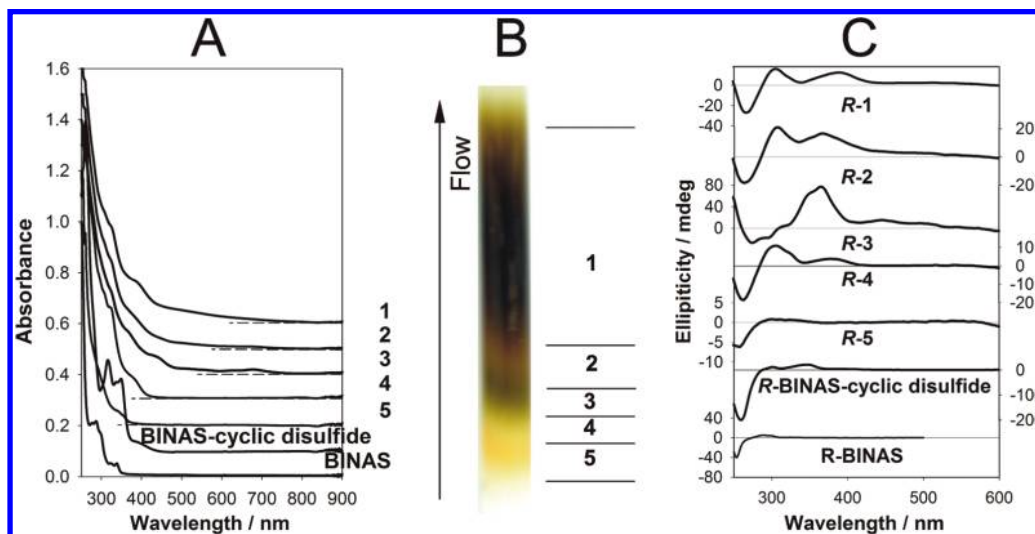


**Figure 1.** (A) UV-vis spectra and (C) ECD spectra of the size-separated nanoparticles 1–5, of (R)-BINAS and of (R)-BINAS-cyclic disulfide. (B) Size exclusion chromatography separation of BINAS protected gold particles. The separated fractions are numbered from 1–5 according to their decreasing elution mobility. Horizontal lines show roughly the limit between adjacent fractions.

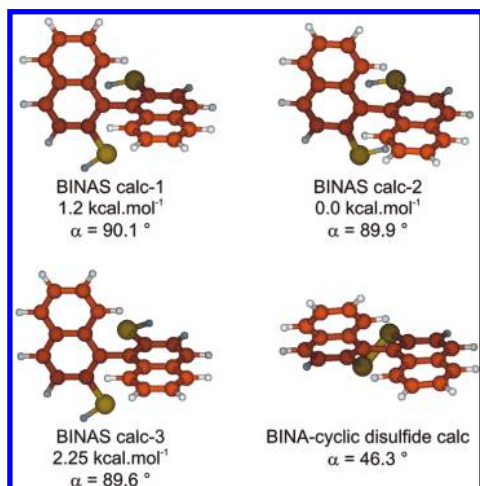


**Figure 2.** Calculated conformers of BINAS and of BINAS-cyclic disulfide. For the BINAS conformers the stability relative to the most stable conformer is also given. The torsion angle  $\alpha$  comprises carbon atoms 2, 1, 1', and 2' (Scheme 1). For computational details see the experimental part.

stable than the ones pointing outward, which might result from electrostatic interactions between these groups. The S–H groups are coplanar to the corresponding naphthyl groups. The angle between the naphthyl groups as measured by the torsion angle  $\alpha$  comprising carbon atoms 2, 1, 1', and 2' (Scheme 1) is in all cases very close to  $90^\circ$ . In contrast, for the cyclic disulfide form the angle  $\alpha$  is only  $46.3^\circ$ . This angle is in good agreement with the torsion angle of  $50.04^\circ$  measured in the solid state by X-ray diffraction (not shown).

For all the structures shown in Figure 2 the IR and VCD spectra were calculated. Table 1 gives a selection of calculated frequencies together with the experimental ones. For the three conformers of BINAS the VCD and IR spectra are very similar (not shown). In the following we therefore concentrate on the vibrational properties of the most stable conformer (BINAS calc-2) only. Figure 3 and Figure 4 show the experimental and calculated IR and VCD spectra of BINAS and BINAS-cyclic disulfide, respectively. The spectra of the two forms are significantly different. Note that the quality of the BINAS-cyclic disulfide VCD spectra is not as good as the one for the dithiol due to the much lower solubility of the former.

**TABLE 1: Calculated and Experimental Wavenumbers ( $\text{cm}^{-1}$ ) of Selected Modes of BINAS, BINAS-Cyclic Disulfide, and BINAS Adsorbed on Gold Nanoparticles<sup>a</sup>**

band	BINAS		BINAS-cyclic disulfide		BINAS Au NPs	
	calc.	exp.	calc.	exp.	calc.	exp.
	1126	1120	1125	1126	1110	
	1128	1133	1135	1139	1119	
	1198	1201				
	1312	1315	1300	1300	1303	1301
	1327	1326	1309		1315	1322
	1356	1350				
4	1439	1447	1436	1450	1432	1438
3	1448	1459	1438		1442	1454
2	1501	1501	1502	1502	1499	1496
1	1505	1507	1504		1503	1508
	1563	1561	1549		1557	1558
	1569	1572	1563		1560	
	1592	1587	1586	1580	1588	1579
	1593		1588		1590	
	1625	1617	1623	1618	1623	1614
	1625		1624		1623	

<sup>a</sup> Bands 1–4 correspond to the modes assigned in the figures.

The VCD spectra of some 1,1'-binaphthyl derivatives have been reported before.<sup>35</sup> There are some bands associated with the binaphthyl core that are characteristic, e.g., bands 1–4 (see Figure 3). The VCD spectrum of BINAS is dominated by pairs of bands with opposite sign. These patterns arise from the splitting of bands due to the  $C_2$  symmetry and the dipolar excitation coupling of the naphthyl chromophores. For example modes 1 and 2 are ring deformation modes localized around C<sub>6</sub>, C<sub>6'</sub>, C<sub>7</sub>, and C<sub>7'</sub> of the binaphthyl part, whereas modes 3 and 4 are localized around C<sub>2</sub> and C<sub>2'</sub> and thus expected to be influenced by substitution at these positions. In general the agreement between experimental and calculated VCD and IR spectra for BINAS is excellent, except for the part below around  $1200\text{ cm}^{-1}$ .

The potential energy surface of the angle  $\alpha$  between the two naphthyl parts is quite shallow and calculations on parent 1,1'-binaphthol have shown that some of the modes in the VCD, including modes 1–4, are quite sensitive to that angle.<sup>35</sup> For example modes 1 and 2 at around  $1500\text{ cm}^{-1}$  can turn from a ( $\pm$ ) couplet at small angles ( $40^\circ$ ) to a ( $\mp$ ) couplet at angles around  $90^\circ$  going through only one single band in between. Also



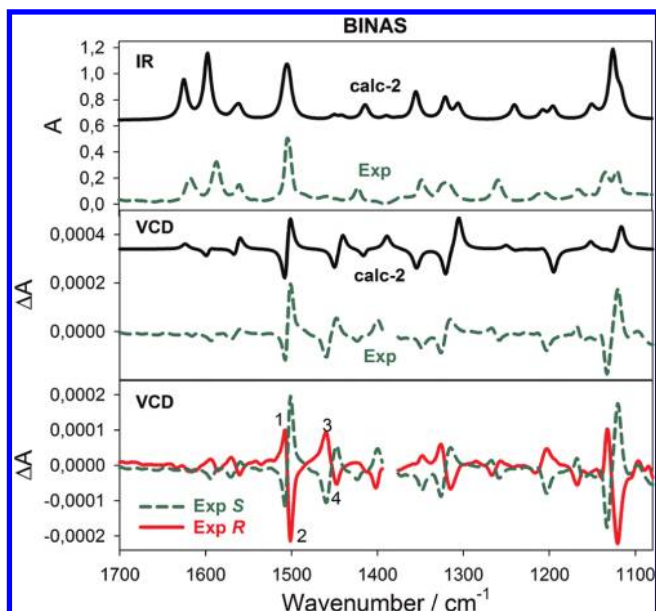


**Figure 3.** Experimental and simulated IR and VCD spectra for BINAS. Calculated spectra for (S)-BINAS calc-2 are plotted in black, experimental spectra for (R)- and (S)-BINAS are plotted in red (solid line) and green (dashed line), respectively. In the experimental VCD spectra the small part below  $1400\text{ cm}^{-1}$  is not accessible due to strong solvent absorption.

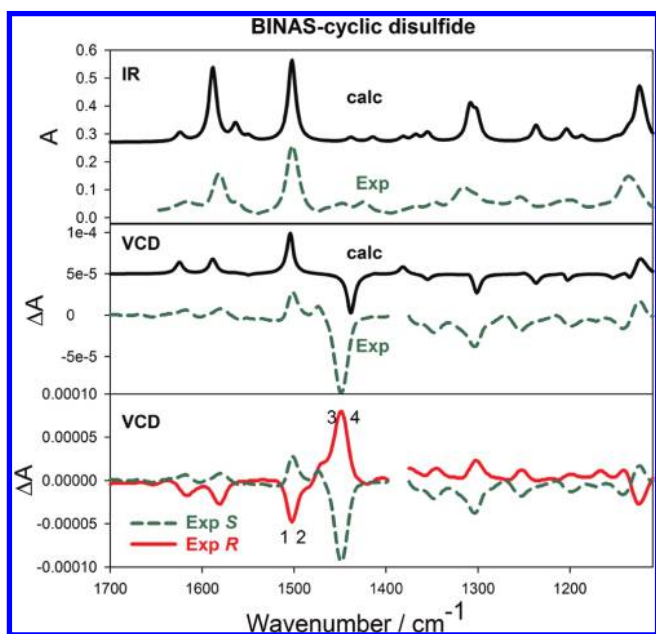


**Figure 4.** Experimental and simulated IR and VCD spectra for BINAS-cyclic disulfide. Calculated spectra for BINAS-cyclic disulfide are plotted in black, experimental spectra for (R)- and (S)-BINAS-cyclic disulfide are plotted in red (solid line) and green (dashed line), respectively. In the experimental VCD spectra the small part below  $1400\text{ cm}^{-1}$  is not accessible due to strong solvent absorption.

modes 3 and 4 can merge into one strong band (negative for (S)-enantiomer) at small angles around  $40^\circ$ . Such behavior is for example observed for BINAS disulfide with a calculated angle of  $46.3^\circ$ . Figure 4 shows that there is only one band in the VCD for modes 1 and 2 and one (strong) with opposite sign for modes 3 and 4. The calculated and experimental IR and VCD spectra are again in excellent agreement. Also the VCD spectrum above about  $1400\text{ cm}^{-1}$  strongly resembles the one reported for 1,1'-binaphthyl-2,2'-diyl-hydrogenphosphate.<sup>35</sup> In the latter the angle between the naphthyl planes is fixed by

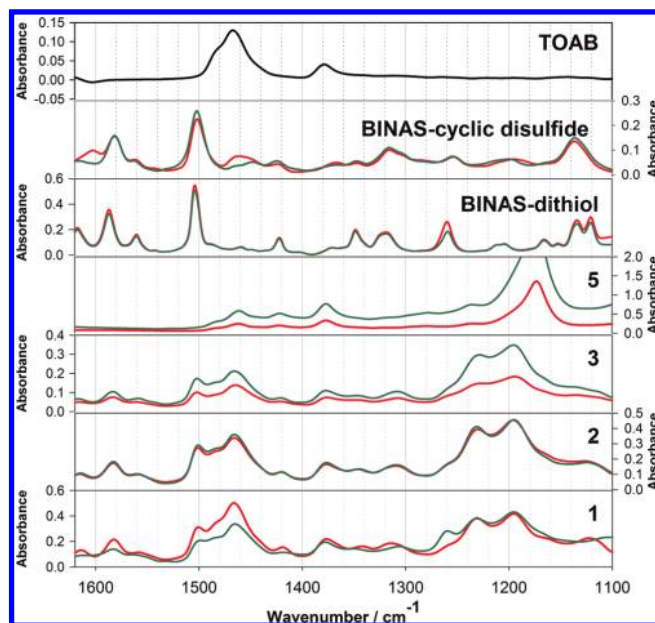


**Figure 5.** Infrared spectra of separated fractions 1–3 and 5 of BINAS-stabilized gold nanoparticles, of BINAS, of BINAS-cyclic disulfide and of TOAB in  $\text{CD}_2\text{Cl}_2$  ( $\text{CDCl}_3$  for BINAS-cyclic disulfide). Red curves and green curves correspond to the (R)- and (S)-enantiomers of the chiral compounds, respectively.

the phosphate bridge at around  $55^\circ$ . In general, the VCD spectra of the dithiol and the disulfide are distinctly different from each other, particularly also for the characteristic modes 1–4.

**BINAS-Stabilized Gold Nanoparticles. IR Spectra.** Figure 5 shows that the IR spectra of the separated fractions 1–3 covered either by the (R)- or the (S)-BINAS are very similar whereas fraction 5 is drastically different. This may be explained by the fact that fraction 5 corresponds to the smaller nanoparticles and this fraction can be polluted by organic residues or Au-thiolate oligomers. The amount of isolated fraction 4 was not high enough to record IR and VCD spectra. The IR spectra of the fractions 1–3 show clearly a superposition of the IR signals of BINAS and TOAB. This result is in good agreement with the  $^1\text{H}$  NMR spectrum of the crude nanoparticles.<sup>16</sup> TOAB is used during the synthesis of the particles as a phase transfer agent<sup>36</sup> and is removable neither by SEC nor by precipitation. TOAB is strongly attached to the particles through charge compensation of the negative gold particles.<sup>37,38</sup> At this stage, a contribution of the BINAS-cyclic disulfide to the IR signal can not be excluded due to the similarity of the IR spectra of both dithiol and disulfide. Surprisingly, the IR spectra of the nanoparticles reveal a strong and broad signal at around  $1200\text{ cm}^{-1}$  which can be attributed neither to the TOAB nor to the two free BINAS forms (dithiol and disulfide). This signal might be explained by the presence of some sulfonate species formed via oxidation of disulfide upon exposure to air in presence of halide ions.<sup>39</sup> However, such species (free sulfate, disulfide and dithiol) have not been evidenced by NMR and might be effectively removed by SEC. Another origin can be a modification of the C–S dipolar moment upon adsorption of the BINAS on gold.

**VCD Spectra.** The VCD spectra of the two enantiomers of BINAS-cyclic disulfide, of BINAS and of BINAS adsorbed on gold nanoparticles 2 show good mirror image relationships and good signal-to-noise ratios as shown in Figure 6. On the one hand, the modes 1–2 and 3–4 of fraction 2 and of BINAS are very similar and form two ( $\pm$ ) couplets whereas the modes 1 and 2 merge in one strong negative band and 3 and 4 merge in

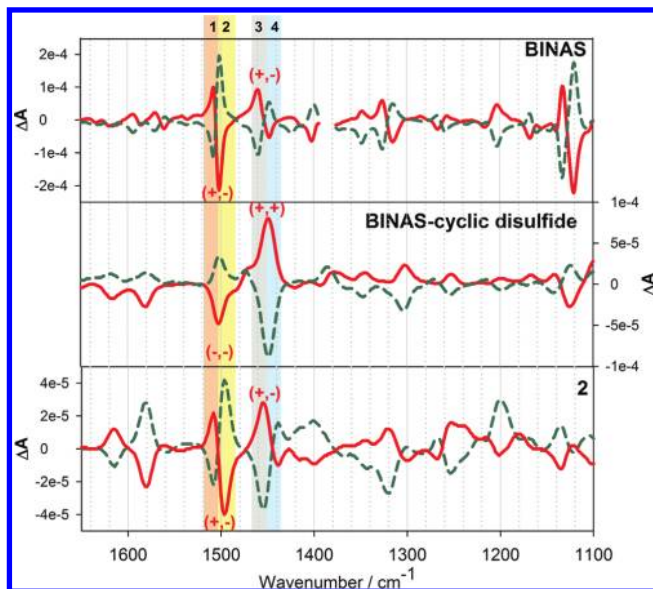


**Figure 6.** VCD spectra of fraction **2** of the size separated nanoparticles protected by the (*R*)- and (*S*)-BINAS, of the free (*R*)- and (*S*)-BINAS, and of the (*R*)- and (*S*)-BINAS-cyclic disulfide. The spectra of the (*R*)- and (*S*)-enantiomers are plotted in red (solid line) and green (dashed line), respectively.

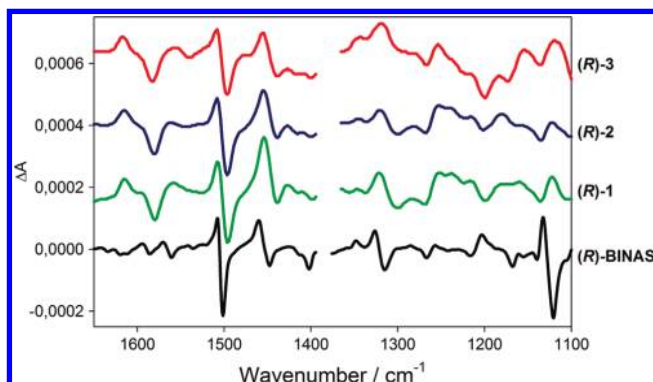


**Figure 7.** VCD spectra of the size-separated nanoparticles protected with (*R*)-BINAS **1–3**. The spectra of the nanoparticles were scaled by a factor of 4.

one strong positive band for (*R*)-BINAS-cyclic disulfide as discussed before. In the case of the particles **2**, the relative intensity of mode 3 with respect to mode 1 is slightly higher than for the BINAS. This can be attributed to a slight reduction of the torsion angle of the BINAS upon adsorption<sup>35</sup> but also only to the contribution of the gold to this mode since this mode is mainly located close to the C<sub>2</sub> and C<sub>2</sub>' atoms which are directly bound to the thiol groups. From the discussion above of bands 1–4 one may conclude that the torsion angle is close to 90° for BINAS adsorbed on gold nanoparticles. On the other hand, the rest of the spectra are largely different for the three compounds in term of sign and intensity. This clearly shows that the vibrational optical activity of the nanoparticle sample does not arise from free BINAS but also that the conformation of the adsorbed BINAS needs to be investigated by DFT calculations (*vide infra*).

Figure 7 shows the VCD spectra of the size separated nanoparticles **1–3** covered with the (*R*)-BINAS and of the free (*R*)-BINAS for comparison. Whereas the size of the particle has strong effects on UV–vis and even more on ECD spectra (see Figure 1), the size has less effects on IR and VCD spectra. Indeed, the different sizes of particles display very similar VCD spectra. The small differences for fraction **3** are rather attributed

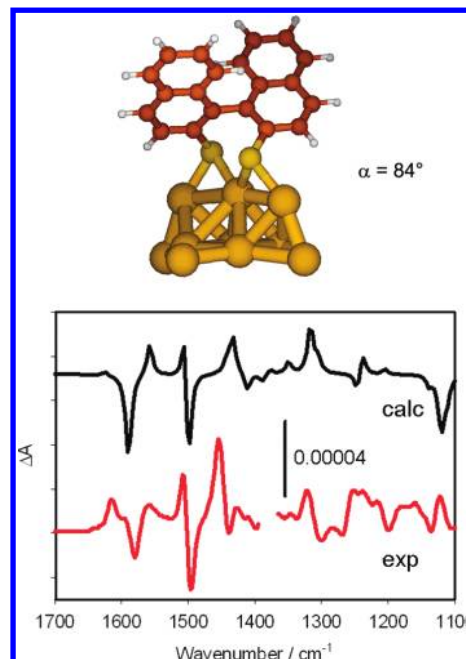


**Figure 8.** Calculated conformer of (*R*)-BINAS adsorbed on a Au<sub>10</sub> cluster. The structure was optimized using Gaussian 03.<sup>40</sup> Simulated VCD spectrum of the calculated conformer of adsorbed (*R*)-BINAS (black) and measured VCD spectrum for the fraction (*R*)-1 (red).

to the lower quality of the spectra due to the smaller quantity of particles available than to a different conformation of the adsorbed BINAS. This result demonstrates that the conformation of the adsorbed dithiol is not drastically modified by the size of the particle even in the subnanometer range. The finding indicates that the vibrational property of the adsorbed molecules is a local property, in contrast to the electronic structure of the particles, as manifested in the UV–vis absorption and CD spectra. The experimental result also justifies the use of models considering only one single adsorbed molecule instead of a whole cluster with several (tens of) molecules for the calculation of VCD spectra.

**DFT Calculations.** We have chosen a Au<sub>10</sub> cluster to study the conformation of adsorbed BINAS. Figure 8 shows the calculated lowest energy conformer of the (*R*)-BINAS adsorbed on the latter cluster. In this conformation, (*R*)-BINAS is adsorbed through the two thiolates. Each thiolate is attached to two gold atoms in a bridge site and one of these two gold atoms is shared between the two thiolates of the BINAS. This adsorption motif, one thiolate adsorbed between two gold atoms with one of the two gold atoms linked to a second thiolate, is similar to the adsorption motif of *p*-mercaptobenzoic acid on a 102 gold atoms nanoparticle which has been determined by Jadzinsky et al. by X-ray diffraction.<sup>41</sup> In that cluster the thiolates are arranged in short staples formed from two thiolates and one gold atom that is detached from the dense gold core. An analogous structural motif was found for Au<sub>25</sub>.<sup>38</sup> In that case the staples are longer, consisting of three thiolates and two detached gold atoms. Both in the short and long staples the S–Au–S bond is nearly linear. Attempts to calculate such structures with BINAS failed. Due to structural constraints there is not enough space for a gold atom to form linear bonds in between the BINAS sulfur atoms. Hence, the BINAS is not compatible with the staple geometry found for monothiolates. In our calculation the gold atom attached to the two thiolates is not detached from the surface and the S–Au–S motif is not linear as in the staple motifs. The torsion angle between the



two naphthyl groups is  $84^\circ$  in our calculated conformation. This angle is relatively close to the torsion angle determined for the free BINAS in solution (vide supra). The simulated spectra for the calculated conformation is in good agreement with the experimental spectrum especially between 1600 and  $1300\text{ cm}^{-1}$  (see Figure 8). The peak in the experimental spectrum at around  $1200\text{ cm}^{-1}$  might originate from sulfonate species (see above). Note that below  $1200\text{ cm}^{-1}$  the VCD measurements are also complicated by lower sensitivity. Indeed, both simulated and experimental spectra, show (+,−) couplets for band 1–2 and 3–4. As discussed before, these signals are strongly dependent on the torsion angle of binaphthyl compounds and characteristic of an angle close to  $90^\circ$  in this case. This reveals that BINAS is not adsorbed in its oxidized (disulfide) form. The strong correlation between the torsion angle determined by DFT calculations and by the qualitative experimental observations of VCD spectra on very similar compounds shows the sensitivity of the DFT-VCD approach for the determination of the conformation of adsorbed molecules on nanoparticles.

It should be noted that the VCD spectra of the adsorbed BINAS is not sensitive to the gold cluster, as long as the geometry of the gold atoms directly bound to the thiolates is not changed. For examples, addition of further gold atoms to the bottom of the cluster shown in Figure 8 has virtually no influence on the VCD spectrum of adsorbed BINAS. On the other hand, adsorbing BINAS on a rigid Au(111) surface cluster model leads to a rather different VCD spectrum.

## Conclusions

Vibrational circular dichroism (VCD) spectra of BINAS adsorbed on small size-separated gold nanoparticles were measured. Calculated VCD spectra of BINAS adsorbed on a simple gold cluster model is in good agreement with the experimental spectra. Both qualitative interpretation based on knowledge of the VCD spectra of binaphthyl compounds and the DFT-VCD approach conclude to a torsion angle close to  $90^\circ$  for BINAS adsorbed on gold clusters. This correlation emphasizes the validity and the sensitivity of the latter approach for the conformational study of absorbates on nanoparticles. The comparison between experimental and calculated spectra furthermore shows that BINAS is not adsorbed in its disulfide form. The VCD spectra of the size separated fractions are very similar. This demonstrates that the conformation of the adsorbed BINAS is not dependent on the size of the nanoparticles and that the vibrational characteristic of the adsorbed molecules is a local property. A better simulation of the structure of the underlying metal atoms may even enhance the correlation between the simulated and the experimental spectra and contribute to a better understanding of the surface reconstruction upon adsorption of organic molecules.

**Acknowledgment.** Financial support by the Swiss National Science Foundation is kindly acknowledged. We thank Prof. S. Gladiali for providing BINAS.

## References and Notes

- (1) Izumi, Y. *Adv. Catal.* **1983**, *32*, 215.
- (2) Orito, Y.; Imai, S.; Niwa, S. *J. Chem. Soc. Jpn.* **1979**, 1118.
- (3) Vargas, A.; Ferri, D.; Bonalumi, N.; Mallat, T.; Baiker, A. *Angew. Chem., Int. Ed.* **2007**, *46*, 3905.
- (4) Bürgi, T.; Baiker, A. *J. Catal.* **2000**, *194*, 445.
- (5) Maris, M.; Bürgi, T.; Mallat, T.; Baiker, A. *J. Catal.* **2004**, *226*, 393.
- (6) Bonalumi, N.; Vargas, A.; Ferri, D.; Bürgi, T.; Mallat, T.; Baiker, A. *J. Am. Chem. Soc.* **2005**, *127*, 8467.
- (7) Bieri, M.; Gautier, C.; Bürgi, T. *Chem. Phys. Phys. Chem.* **2007**, *9*, 671.
- (8) Nafie, L. A.; Keiderling, T. A.; Stephens, P. J. *J. Am. Chem. Soc.* **1976**, *98*, 2715.
- (9) Nafie, L. A. *Annu. Rev. Phys. Chem.* **1997**, *48*, 357.
- (10) Gautier, C.; Bürgi, T. *Chem. Commun.* **2005**, *43*, 5393.
- (11) Gautier, C.; Bürgi, T. *J. Am. Chem. Soc.* **2006**, *128*, 11079.
- (12) Bieri, M.; Bürgi, T. *J. Phys. Chem. B* **2005**, *109*, 22476.
- (13) Nafie, L. A. *J. Phys. Chem. A* **2004**, *108*, 7222.
- (14) Hartsein, A.; Kirtley, J. R.; Tsang, J. C. *Phys. Rev. Lett.* **1980**, *45*, 201.
- (15) Jalkanen, K. J.; Degtyarenko, I. M.; Nieminen, R. M.; Cao, X.; Nafie, L. A.; Zhu, F.; Barron, L. D. *Theor. Chem. Acc.* **2008**, *119*, 191.
- (16) Gautier, C.; Taras, R.; Gladiali, S.; Bürgi, T. *Chirality* **2008**, *20*, 486.
- (17) Fabbri, D.; Delogu, G.; De Lucchi, O. *J. Org. Chem.* **1993**, *58*, 1748.
- (18) Becke, A. D. *J. Chem. Phys.* **1993**, *98*, 5648.
- (19) Perdew, J. P.; Chevary, J. A.; Vosko, S. H.; Jackson, K. A.; Pederson, M. R.; Singh, D. J.; Fiolhais, C. *Phys. Rev. B* **1992**, *46*, 6671.
- (20) Hay, P. J.; Wadt, W. R. *J. Chem. Phys.* **1985**, *82*, 270.
- (21) Ditchfield, R.; Hehre, W. J.; Pople, J. A. *J. Chem. Phys.* **1971**, *54*, 724.
- (22) Schaaff, T. G.; Whetten, R. L. *J. Phys. Chem. B* **2000**, *104*, 2630.
- (23) Tamura, M.; Fujihara, H. *J. Am. Chem. Soc.* **2003**, *125*, 15742.
- (24) Gautier, C.; Bieri, M.; Dolamic, I.; Angeloni, S.; Boudon, J.; Bürgi, T. *Chimia* **2006**, *60*, 777.
- (25) Yanagimoto, Y.; Negishi, Y.; Fujihara, H.; Tsukuda, T. *J. Phys. Chem. B* **2006**, *110*, 11611.
- (26) Shemer, G.; Krichavski, O.; Markovich, G.; Molotsky, T.; Lubitz, I.; Kotlyar, A. B. *J. Am. Chem. Soc.* **2006**, *128*, 11006.
- (27) Negishi, Y.; Tsunoyama, H.; Suzuki, M.; Kawamura, N.; Matsushita, M. M.; Maruyama, K.; Sugawara, T.; Yokoyama, T.; Tsukuda, T. *J. Am. Chem. Soc.* **2006**, *128*, 12034.
- (28) Gautier, C.; Bürgi, T. *J. Am. Chem. Soc.* **2008**, *130*, 7077.
- (29) Yao, H. *Curr. Nanosci.* **2008**, *4*, 92.
- (30) Gautier, C.; Bürgi, T. *Chiral Nanoparticles. In Chirality at the Nanoscale: Nanoparticles, Surfaces, Materials and more*; Amabilino, D. B., Ed.; Wiley-VCH: Weinheim, 2009; Vol. 1, pp 380.
- (31) Hidalgo, F.; Sanchez-Castillo, A.; Garzón, I. L.; Noguez, C. *Eur. Phys. J. D* **2009**, *52*, 179.
- (32) Noguez, C.; Garzón, I. L. *Chem. Soc. Rev.* **2009**, *38*, 757.
- (33) Gautier, C.; Bürgi, T. *ChemPhysChem* **2009**, *10*, 483.
- (34) Si, S.; Gautier, C.; Boudon, J.; Taras, R.; Gladiali, S.; Bürgi, T. *J. Phys. Chem. C* **2009**, *113*, 12966.
- (35) Setnicka, V.; Urbanova, M.; Bour, P.; Kral, V.; Volka, K. *J. Phys. Chem. A* **2001**, *105*, 8931.
- (36) Brust, M.; Walker, M.; Bethell, D.; Schiffrin, D. J.; Whyman, R. *J. Chem. Soc., Chem. Commun.* **1994**, 801.
- (37) Price, R. C.; Whetten, R. L. *J. Am. Chem. Soc.* **2005**, *127*, 13750.
- (38) Heaven, M. W.; Dass, A.; White, P. S.; Holt, K. M.; Murray, R. W. *J. Am. Chem. Soc.* **2008**, *130*, 3754.
- (39) Dasog, M.; Scott, R. W. *J. Langmuir* **2007**, *23*, 3381.
- (40) Frisch, M. J.; et al. *Gaussian 03*, revision C.01; Gaussian, Inc.: Wallingford, CT, 2003.
- (41) Jadzinsky, P. D.; Calero, G.; Ackerson, C. J.; Bushnell, D. A.; Kornberg, R. D. *Science* **2007**, *318*, 430.

JP910800M